

AIAA 81-4214

# Procedure for Obtaining Aerodynamic Properties of Spacecraft

Richard M. Fredo\* and Marshall H. Kaplan†

*The Pennsylvania State University, University Park, Penna.*

A numerical procedure for calculating free-molecular aerodynamic coefficients for a large class of spacecraft configurations is presented. This involves modeling the spacecraft via the use of basic geometric shapes. The surface of each shape is numerically divided into small elemental areas. Overall coefficients are determined by summing force contributions from each of the exposed surface elements. Surface shielding is accounted for through the use of a shadow-projection technique and simple geometric relationships. Forces on elemental areas are determined by using the gas-surface interaction model attributed to Schaaf and Chambre with experimental momentum accommodation data. The procedure is implemented as a computer program. To illustrate the use and accuracy of this procedure, it is applied to the complex Skylab configuration. Results are compared with analytical predictions from a previous study.

## Nomenclature

|                          |  |                                      |   |
|--------------------------|--|--------------------------------------|---|
| $A_e$                    | = area of surface element  | $T_w$                                | = average spacecraft surface temperature  |
| $A_{ref}$                | = spacecraft reference area  | $u, v, w$                            | = $X_e, Y_e,$ and $Z_e$ components of the absolute molecular velocity   |
| $C_D$                    | = overall drag coefficient   | $\bar{U}, U$                         | = relative macroscopic velocity vector and its magnitude between the spacecraft and the incident molecular flux |
| $C_{Fx}, C_{Fy}, C_{Fz}$ | = overall force coefficients in the $X_B, Y_B,$ and $Z_B$ directions   | $U_x, U_y, U_z$                      | = components of velocity $U$ along $X_B, Y_B, Z_B$ axes   |
| $C_{Mx}, C_{My}, C_{Mz}$ | = overall moment coefficients about the $X_B, Y_B,$ and $Z_B$ axes   | $x_0, y_0, z_0$                      | = $X_B, Y_B,$ and $Z_B$ components of the position of the origin of the component system of a basic shape       |
| $C_{XB}, C_{YB}, C_{ZB}$ | = force coefficients in the $X_B, Y_B,$ and $Z_B$ directions for a single surface element  | $X_A, Y_A, Z_A$                      | = aerodynamic system coordinates  |
| $d_{XC}, d_{YC}, d_{ZC}$ | = position components of the centroid of a surface element in the component system of the shape involved in a position comparison with the element | $X_B, Y_B, Z_B$                      | = body system coordinates   |
| $D_c$                    | = distance between the centroid of a surface element and the flowline intersection point   | $X_C, Y_C, Z_C$                      | = component system coordinates  |
| $D_p$                    | = panel dimension  | $X_e, Y_e, Z_e$                      | = elemental system coordinates  |
| $e$                      | = direction cosine matrix that locates the $X_e, Y_e,$ and $Z_e$ axes of an element with respect to the $X_C, Y_C,$ and $Z_C$ axes                 | $\epsilon_x, \epsilon_y, \epsilon_z$ | = direction cosines that locate the flow direction with respect to the $X_e, Y_e,$ and $Z_e$ axes               |
| $f$                      | = molecular distribution function  | $\delta_x, \delta_y, \delta_z$       | = angles between the flow direction and the $X_C, Y_C,$ and $Z_C$ axes of a basic shape                         |
| $F_{Xe}, F_{Ye}, F_{Ze}$ | = forces on a surface element in the $X_e, Y_e,$ and $Z_e$ directions  | $\theta$                             | = aerodynamic angle of attack   |
| $k$                      | = Boltzman constant  | $\theta_i$                           | = incidence angle   |
| $l$                      | = direction cosine matrix that locates the $X_C, Y_C,$ and $Z_C$ axes with respect to the body coordinate system                                   | $\rho$                               | = mass density  |
| $L_{ref}$                | = spacecraft reference length  | $\sigma_n, \sigma_t$                 | = normal and tangential momentum accommodation coefficients   |
| $m$                      | = mass of an atmospheric molecule  | $\tau$                               | = net shear on a surface element  |
| $\bar{n}$                | = unit vector normal to a surface element  | $\tau_i$                             | = shear due to incident molecular flux  |
| $p$                      | = net pressure on surface element  | $\phi$                               | = aerodynamic roll angle  |
| $p_i$                    | = pressure due to incident molecular flux  |                                      |   |
| $p_w$                    | = pressure exerted by molecules reemitted from surface in Maxwellian equilibrium at the surface temperature  |                                      |   |
| $P_{XC}, P_{YC}, P_{ZC}$ | = components of the position of the centroid of an element in the component system of the basic shape to which the element belongs                 |                                      |   |
| $S$                      | = molecular speed ratio  |                                      |   |
| $T$                      | = atmospheric temperature (freestream temperature)   |                                      |   |

## Introduction

**A** PREREQUISITE for the prediction of near-Earth satellite motion is the determination of free-molecular aerodynamic forces and moments. Such forces and moments are defined in terms of aerodynamic coefficients which are functions of spacecraft geometry, attitude, orbital velocity, and the mechanics of the interaction between the rarefied atmosphere and satellite surfaces. A numerical procedure to calculate these coefficients for a wide range of spacecraft configurations is presented.

A problem that arises in the determination of aerodynamic coefficients is that of modeling the gas-surface interaction. When the early satellites were placed in orbit, only limited information on these interactions was available. Therefore, drag coefficients were often estimated by assuming that the incident molecules were diffusely reemitted with perfect energy accommodation. Experimental studies have shown that these assumptions are not completely valid for the satellite environment.

Received July 2, 1980; revision received Feb. 27, 1981. Copyright ©

\*Graduate Assistant, Department of Aerospace Engineering. Presently with Lockheed Missiles and Space Company, Sunnyvale, Calif. Member AIAA.

†Professor of Aerospace Engineering. Associate Fellow AIAA.

An interaction model<sup>1</sup> that has been frequently used for aerodynamic calculations incorporates two accommodation coefficients to define the degree of momentum exchange between the incident molecular flux and the satellite surface. Past users<sup>2,4</sup> of this model assumed that the accommodation coefficients were constants. Experimental studies<sup>5,6</sup> have shown that these coefficients vary widely with incidence angle and incident particle energy.

Another problem that complicates the determination of the aerodynamic coefficients is that of surface shielding. In free-molecular flow, a situation often arises in which a portion of a spacecraft is shielded from the incident flow by other parts of the spacecraft. This effect is normally experienced by spacecraft that utilize solar arrays, dish antennas, and other extended appendages. Since shielded surfaces do not experience significant forces, the outline of the shielded regions must be known in order to accurately determine the overall aerodynamic coefficients.

The early satellites were of such simple geometry that shielding was not a problem. The development of "paddlewheel" satellites, however, presented the aerodynamicist with the task of determining the outline of the shielded main-body regions. Because of the symmetrical geometry of these satellites, analytical expressions can be derived that define the shape of the shielded regions as functions of the satellite attitude and geometry. With the development of complex, asymmetric configurations such as Skylab, it is impractical to derive analytical expressions to define shielded-region outlines. Therefore, numerical approaches have been developed.

The main points of the procedure include:

- 1) Spacecraft configurations are modeled as a combination of basic geometric shapes by defining the type, dimensions, and orientation of each element utilized in the model. Flowfield data (molecular speed ratio, average temperature ratio, etc.) are also assigned.
- 2) Once the spacecraft attitude relative to the incident flow has been defined, the surfaces of the configuration are divided into numerous elemental areas.
- 3) These surface elements are checked individually for their flowfield status (exposed or shielded). A shadow-projection technique and simple geometric relationships are utilized for status determination.
- 4) Elemental forces are computed for the elements exposed to the flow. These forces are determined by using the gas-surface interaction model of Schaaf and Chambre<sup>1</sup> and the momentum accommodation data of Knechtel and Pitts.<sup>6</sup>
- 5) The overall force and moment coefficients are determined by summing the elemental force contributions for all the exposed elements.

## Spacecraft Configuration Modeling

### Coordinate Systems and Geometric Shapes

The attitude of a spacecraft is defined in the aerodynamic coordinate system represented by  $X_A$ ,  $Y_A$ , and  $Z_A$  as shown in Fig. 1. The  $Y_A$  axis points in the direction of the relative velocity  $\bar{U}$  between the atmospheric molecules and the spacecraft.  $X_B$ ,  $Y_B$ , and  $Z_B$  define a body coordinate system. These axes are fixed to the spacecraft. The transformation from body system to aerodynamic system is a simplified form of the basic Euler transformation<sup>7</sup>

$$\begin{bmatrix} X_A \\ Y_A \\ Z_A \end{bmatrix} = \begin{bmatrix} \cos\phi & -\sin\phi & 0 \\ \sin\phi\cos\theta & \cos\phi\cos\theta & -\sin\theta \\ \sin\phi\sin\theta & \cos\phi\sin\theta & \cos\theta \end{bmatrix} \begin{bmatrix} X_B \\ Y_B \\ Z_B \end{bmatrix} \quad (1)$$

The angle of attack  $\theta$  used here is not the more common "angle of attack." Thus, it may be helpful to note the transformation from  $\theta$ ,  $\phi$  to body-oriented components of

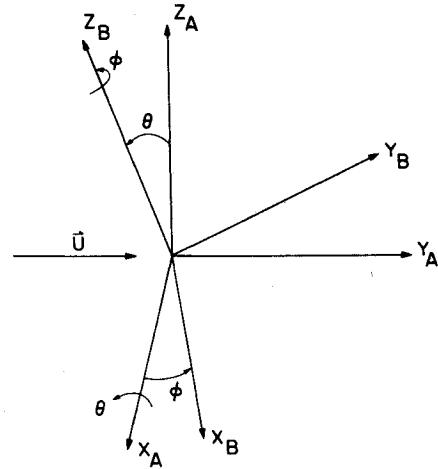


Fig. 1 Aerodynamic and body coordinate systems.

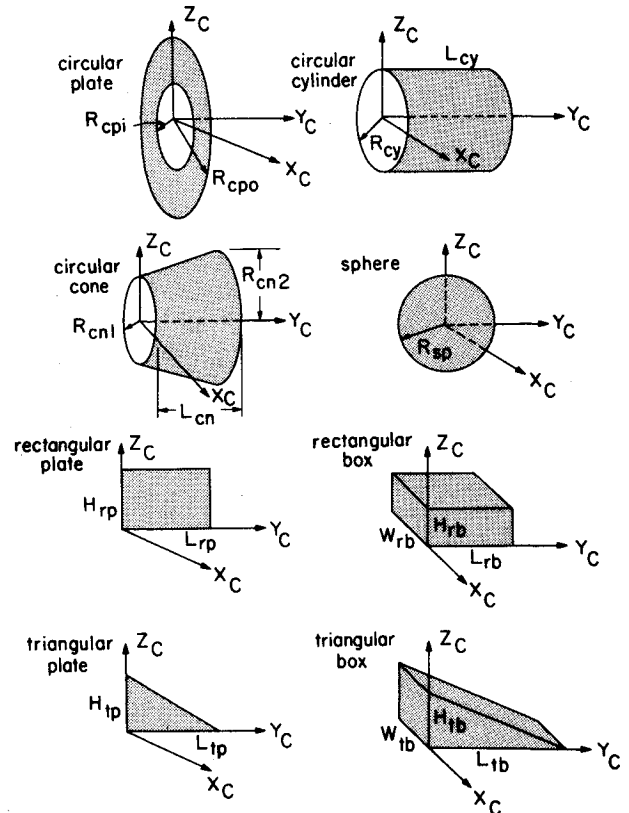


Fig. 2 Basic shapes and component coordinate systems.

velocity

$$U_x = U \sin\phi \cos\theta$$

$$U_y = U \cos\phi \cos\theta$$

$$U_z = -U \sin\theta$$

The angle of attack  $\theta$  is then  $\arcsin(-U_z/U)$  and the aerodynamic roll angle  $\phi$  is  $\arctan(U_x/U_y)$ , with roll equal to zero when  $U_x = 0$ .

A spacecraft is modeled by superimposing onto the body coordinate system any appropriate number of the basic geometric shapes shown in Fig. 2. The  $X_C$ ,  $Y_C$ , and  $Z_C$  axes fixed to each of the basic shapes is referred to as the component coordinate system.

The transformation from a component system to the body system is expressed by

$$\begin{bmatrix} X_B \\ Y_B \\ Z_B \end{bmatrix} = \begin{bmatrix} x_0 \\ y_0 \\ z_0 \end{bmatrix} + I \begin{bmatrix} X_C \\ Y_C \\ Z_C \end{bmatrix} \quad (2)$$

where  $x_0$ ,  $y_0$ , and  $z_0$  define the position of the origin of the component system in the body system. The direction cosine matrix  $I$  locates the  $X_C$ ,  $Y_C$ , and  $Z_C$  axes of a basic shape with respect to the body system.

#### Elemental Surface Division

Overall aerodynamic coefficients are determined by dividing each spacecraft surface into numerous elemental areas and then summing the contributions from each exposed element.

The aerodynamic forces on a surface element are assumed to act at the element centroid. For each element, the centroid position is defined in terms of the geometry of the basic shape. A coordinate system referred to as the elemental system is defined at the centroid of each element for specifying the direction of the elemental forces. The direction cosine matrix  $e$  that locates the elemental system with respect to the component system is also specified according to the surface geometry. The direction and point of application of the elemental forces is now definable in the body coordinate system.

#### Exposure Determination

##### Shadow-Projection Technique

As pointed out above, a situation often arises in which components are shielded from the flow by other parts of the spacecraft. Since shielded surfaces do not experience significant forces, such regions must be determined to accurately calculate overall coefficients. The flowfield status (exposure or nonexposure) of a surface element is determined from a comparison of its position with respect to positions of all other basic shapes that make up the spacecraft configuration. For a complex configuration that is composed of 20 or 30 shapes and thousands of surface elements, the status determination for all the elements would require a large amount of computer time. A projection technique that can reduce the number of element-shape comparisons is now briefly described.

This technique involves the projection of the spacecraft configuration onto a square flat panel that is perpendicular to the  $Y_A$  axis and divided into numerous regions as shown in Fig. 3. In this example, the number of panel divisions is equal to 10. The panel dimension  $D_p$  is defined as the distance between the body-system origin and the point on the surface of the configuration farthest from the origin. The panel dimension is defined in this manner to insure that the spacecraft projection will lie completely within the panel boundaries. For the CSM configuration shown in the figure, the farthest point from the body-system origin is denoted by 0.

The projection of the spacecraft geometry is done by representing each of the basic shapes as a set of points and then projecting these points onto the panel. A rectangular plate is modeled with four points, one point at each corner of the plate. A circular plate is represented as a polygon by using 16 points equally spaced along the plate's outer perimeter. The other basic shapes are modeled in a similar manner.

The  $X_A$  position components of the projected points for each shape are then compared in order to determine the regions partially obscured by each shape's projection. For example, for shape No. 3 (cylinder) in Fig. 3, the points with the smallest and largest  $X_A$  components are denoted by A and B. Since points A and B are located in regions 4 and 8, respectively, the cylinder obscures parts of regions 4, 5, 6, 7, and 8.

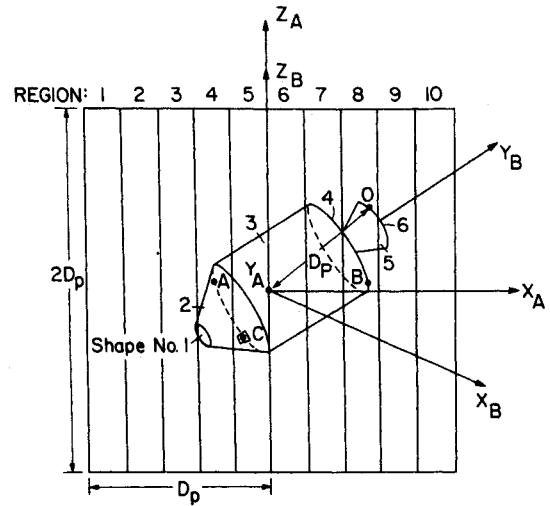


Fig. 3 Shadow-projection panel.

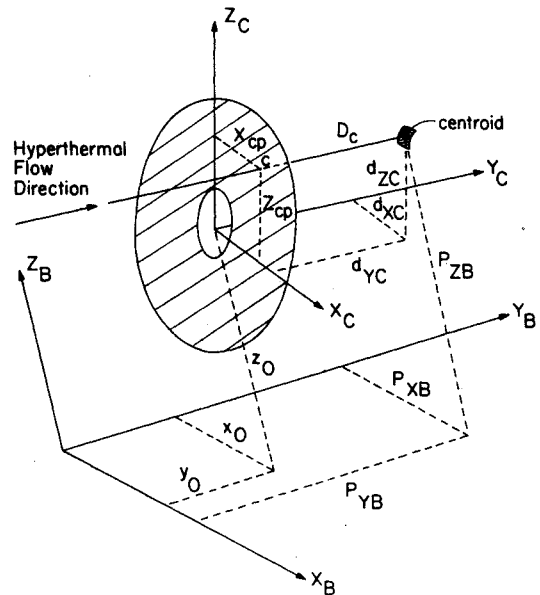


Fig. 4 Element-circular plate position comparison.

The number of element-shape comparisons is reduced using the projection technique since an element's position is to be compared with the position of only those shapes whose projections partially obscure the panel region in which the element is located. For example, the conical element denoted by C in Fig. 3 is located in region 5 which is partially obscured by shapes 2 and 3. Since the element belongs to shape 2, its flowfield status is determined by comparing its position with the position of only shape No. 3 (cylinder).

#### Shielding Analysis

Random thermal motion of molecules can be neglected (hypersonic flow), facilitating the analysis of position comparisons between a surface element and each basic shape. Thus, incident molecular flux is similar to a light beam in the nature in which shadows are cast. A surface element is considered shielded if the position of its centroid lies within the "shadow" cast by a basic shape. It can be determined from the work of Fan<sup>8</sup> that hypersonic shielding is a good approximation when the molecular speed ratio is greater than 5.0.

A surface element in the vicinity of a circular plate is shown in Fig. 4. The position of the element's centroid in the plate's

component system is given by

$$\begin{bmatrix} d_{XC} \\ d_{YC} \\ d_{ZC} \end{bmatrix} = (I_{cp})^T \begin{bmatrix} P_{XB} - x_0 \\ P_{YB} - y_0 \\ P_{ZB} - z_0 \end{bmatrix} \quad (3)$$

where  $P_{XB}$ ,  $P_{YB}$ , and  $P_{ZB}$  are given by

$$\begin{bmatrix} P_{XB} \\ P_{YB} \\ P_{ZB} \end{bmatrix} = I_{es} \begin{bmatrix} P_{XC} \\ P_{YC} \\ P_{ZC} \end{bmatrix} \quad (4)$$

The subscripts  $cp$  and  $es$  refer to the circular plate and the shape to which the element belongs, respectively. Components  $P_{XC}$ ,  $P_{YC}$ , and  $P_{ZC}$  define the position of the element's centroid in the component coordinate system of the basic shape identified by  $es$ . The distance from the element centroid to point  $c$  is defined by

$$D_c = d_{YC} / \cos \delta_Y \quad (5)$$

where  $\delta_Y$  is the angle between the flow direction and the  $Y_C$  axis of the plate. Point  $c$  identifies the intersection of the  $X_C - Z_C$  plane by a flowline that passes through the centroid of the surface element. The value of  $D_c$  is positive when the surface element is downstream of point  $c$  (as in Fig. 4) and negative when the element is located upstream of point  $c$ . For the downstream case, the position of the flowline intersection point in the plate's component system is given by

$$X_{cp} = d_{XC} - D_c \cos \delta_X$$

$$Y_{cp} = 0.0$$

$$Z_{cp} = d_{ZC} - D_c \cos \delta_Z$$

The surface element is shielded from the flow if point  $c$  is located on the plate as is shown in Fig. 4. Therefore, the element is exposed if either of the following conditions is satisfied:

$$(X_{cp}^2 + Z_{cp}^2)^{1/2} > R_{cpo}$$

$$(X_{cp}^2 + Z_{cp}^2)^{1/2} < R_{cpi}$$

The shielding conditions for a rectangular or triangular plate or box are determined in a similar manner.

A surface element located near a circular cylinder is shown in Fig. 5. A flowline passing through the cylinder intersects the surface at two points,  $c_1$  and  $c_2$ . The distances,  $D_{c1}$  and  $D_{c2}$ , are related to the surface geometry by a quadratic equation. The equation is expressed as

$$(\cos^2 \delta_X + \cos^2 \delta_Z) D_c^2 - 2(d_{XC} \cos \delta_X + d_{ZC} \cos \delta_Z) D_c + d_{XC}^2 + d_{ZC}^2 - R_{cy}^2 = 0 \quad (6)$$

where the roots of the equation are  $D_{c1}$  and  $D_{c2}$ . These roots are positive when the surface element is located downstream of points  $c_1$  and  $c_2$  (as in Fig. 5) and negative when the element is upstream of  $c_1$  and  $c_2$ . Also, the element is exposed if the roots are imaginary. This condition, given as

$$(2d_{XC} \cos \delta_X + 2d_{ZC} \cos \delta_Z)^2 < 4(\cos^2 \delta_X + \cos^2 \delta_Z) [d_{XC}^2 + d_{ZC}^2 - R_{cy}^2] \quad (7)$$

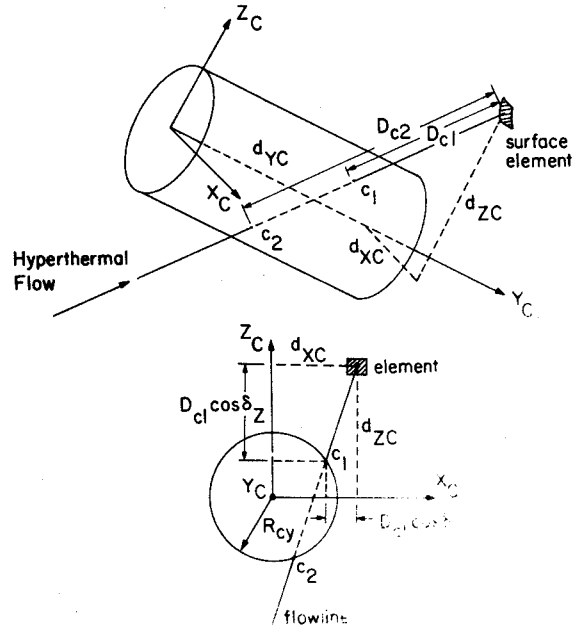


Fig. 5 Element-cylinder position comparison.

signifies that the flowline does not intersect the cylindrical surface. If the roots  $D_{c1}$  and  $D_{c2}$  are positive, the element is exposed only if one of the following conditions is satisfied by both of the roots:

$$d_{YC} - D_c \cos \delta_Y < 0 \quad d_{YC} - D_c \cos \delta_Y > L_{cy} \quad (8)$$

The conditions for a circular cone and sphere are developed in a similar manner.

Each exposed surface element must satisfy the condition

$$\bar{U} \cdot \bar{n} \geq 0 \quad (9)$$

This implies that a surface element is on the windward side of a basic shape.

### Free-Molecular Forces

Atmospheric molecules striking a spacecraft surface are assumed to be in Maxwellian equilibrium. Therefore, the molecular distribution function has the form

$$f = \frac{\rho}{m} \left( \frac{m}{2\pi kT} \right)^{3/2} \exp \left\{ -\frac{m}{2kT} [(u - U_{\epsilon_x})^2 + (v - U_{\epsilon_y})^2 + (w - U_{\epsilon_z})^2] \right\} \quad (10)$$

where velocity vector  $\bar{U}$  defines the motion of the incident molecular flux relative to a spacecraft surface element. The  $X_e$ ,  $Y_e$ , and  $Z_e$  components of  $\bar{U}$  are defined as  $U_{\epsilon_x}$ ,  $U_{\epsilon_y}$ , and  $U_{\epsilon_z}$ .

The force on a surface element in the  $X_e$  direction is simply the product of the net pressure  $p$  and the elemental area  $A_e$ . According to Schaaf and Chambre<sup>1</sup> the net pressure can be expressed as

$$p = (2 - \sigma_n) p_i + \sigma_n p_w \quad (11)$$

Pressure  $p_w$  exerted by the molecules reemitted from the surface with only a Maxwellian random motion corresponding to the surface temperature  $T_w$  is defined as

$$p_w = \frac{1}{2} m \left( \frac{2\pi kT_w}{m} \right)^{1/2} \int_{-\infty}^{\infty} \int_{-\infty}^{\infty} \int_0^{\infty} u f du dv dw \quad (12)$$

Pressure  $p_i$  due to the incident molecular flux is expressed as

$$p_i = m \int_{-\infty}^{\infty} \int_{-\infty}^{\infty} \int_0^{\infty} u^2 f du dv dw \quad (13)$$

By combining Eqs. (10-13) and integrating over velocity half-space, the force on a surface element in the  $X_e$  direction is expressed as

$$F_{Xe} = \frac{\rho A_e U^2}{2S^2} \left( \left[ \frac{2-\sigma_n}{\pi^{1/2}} S \epsilon_x + \frac{\sigma_n}{2} \left( \frac{T_w}{T} \right)^{1/2} \right] \exp[-(S \epsilon_x)^2] + \left\{ (2-\sigma_n) [1/2 + (S \epsilon_x)^2] + \frac{\sigma_n}{2} \left( \frac{T_w \pi}{T} \right)^{1/2} S \epsilon_x \right\} [1 + \operatorname{erf}(S \epsilon_x)] \right) \quad (14)$$

where  $S$  is the molecular speed ratio defined as

$$S = \frac{U}{[2(k/m)T]^{1/2}} \quad (15)$$

The force component in the  $Y_e$  direction is simply the product of the  $Y_e$  component of the net shear and the elemental area  $A_e$ . The net shear is defined as

$$\tau = \sigma_t \tau_i \quad (16)$$

The  $Y_e$  component of shear due to the incident molecular flux is given by

$$(\tau_i)_{Y_e} = m \int_{-\infty}^{\infty} \int_{-\infty}^{\infty} \int_0^{\infty} uv f du dv dw \quad (17)$$

Therefore, combining Eqs. (10), (16), and (17) and integrating, the force  $F_{Ye}$  is given as

$$F_{Ye} = \frac{\rho A_e U^2 \sigma_t}{2S^2 \pi^{1/2}} \{ S \epsilon_y \exp[-(S \epsilon_x)^2] + \pi^{1/2} \epsilon_x \epsilon_y S^2 [1 + \operatorname{erf}(S \epsilon_x)] \} \quad (18)$$

Similarly, the force on the surface element in the  $Z_e$  direction is given by

$$F_{Ze} = \frac{\rho A_e U^2 \sigma_t}{2S^2 \pi^{1/2}} \{ S \epsilon_z \exp[-(S \epsilon_x)^2] + \pi^{1/2} \epsilon_x \epsilon_z S^2 [1 + \operatorname{erf}(S \epsilon_x)] \} \quad (19)$$

These forces,  $F_{Xe}$ ,  $F_{Ye}$ , and  $F_{Ze}$ , are highly dependent on the accommodation coefficients  $\sigma_n$  and  $\sigma_t$ . Knechtel and Pitts<sup>6</sup> have experimentally determined these coefficients for the interaction of nitrogen ( $N_2$ ) on an aluminum surface at various incidence angles and gas energies. Their results are considered valid for spacecraft interacting with the atmosphere below 300 km. This is because  $N_2$  accounts for the major momentum contribution to spacecraft below this altitude.

The results of Knechtel and Pitts for a gas energy range of 8 to 10 eV are used in the present study. This energy range corresponds to an orbital velocity range of 7.4 to 8.3 km/s. Within this range,  $\sigma_n$  and  $\sigma_t$  were found to be more sensitive to a variation in incidence angle than a change in orbital velocity. Values of  $\sigma_n$  and  $\sigma_t$  as functions of  $\theta_i$  are shown in Figs. 6 and 7. To facilitate the aerodynamic calculations, the experimental results of these figures are approximated by

$$\begin{aligned} \sigma_n &= 0.93 - 1.48 \times 10^{-3} \theta_i - 7.00 \times 10^{-5} \theta_i^2 \\ \sigma_t &= 0.63 [1.00 - \exp(-3.38 \times 10^{-2} \theta_i)] \end{aligned} \quad (20)$$

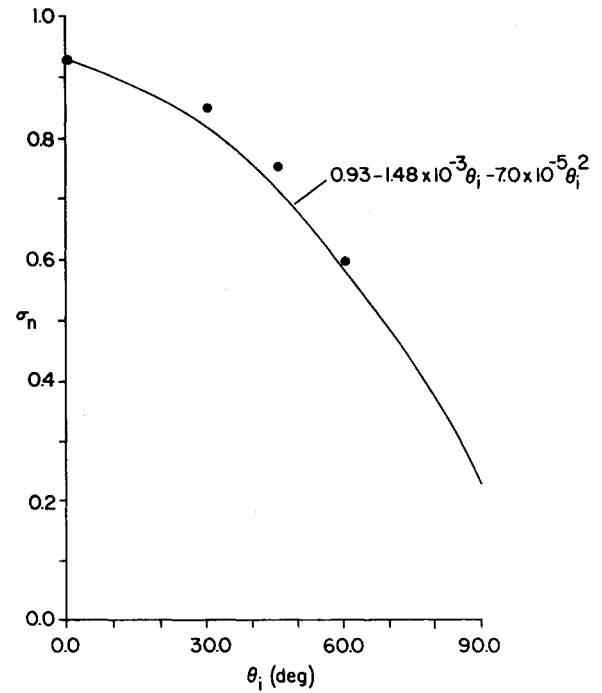


Fig. 6 Normal momentum accommodation coefficient for  $N_2$  on Al as a function of incidence angle.

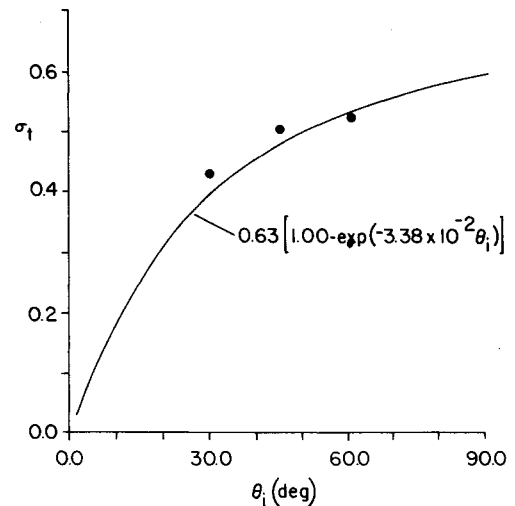


Fig. 7 Tangential momentum accommodation coefficient for  $N_2$  on Al as a function of incidence angle.

where  $\theta_i$  is in degrees. These equations are not the result of an exact curve-fitting analysis, but are sufficient to represent the variation of the accommodation coefficients with incidence angle. The uncertainty associated with the experimental results negates the use of an exact curve-fitting analysis.

#### Overall Coefficients

Overall force and moment coefficients are determined by summing the contributions for all of the exposed surface elements and then normalizing by an appropriate reference area  $A_{ref}$  and reference length  $L_{ref}$ . The force coefficients are defined as

$$C_{Fx} = \sum_{i=1}^I \sum_{j=1}^{J(i)} (C_{XB} A_e)_{ij} (A_{ref})^{-1} \quad (21a)$$

$$C_{Fy} = \sum_{i=1}^I \sum_{j=1}^{J(i)} (C_{YB} A_e)_{ij} (A_{ref})^{-1} \quad (21b)$$

$$C_{Fz} = \sum_{i=1}^I \sum_{j=1}^{J(i)} (C_{ZB} A_e)_{ij} (A_{ref})^{-1} \quad (21c)$$

where  $i$  identifies the basic shape and  $j$  identifies the surface element. The parameters  $I$  and  $J$  represent the total number of basic shapes and the total number of elements per shape, respectively. The coefficients  $C_{XB}$ ,  $C_{YB}$ , and  $C_{ZB}$ , for an arbitrary element on an arbitrary basic shape, are given as

$$\begin{bmatrix} C_{XB} \\ C_{YB} \\ C_{ZB} \end{bmatrix} = Ie \begin{bmatrix} C_{Xe} \\ C_{Ye} \\ C_{Ze} \end{bmatrix} \quad (22)$$

where the elemental force coefficients  $C_{Xe}$ ,  $C_{Ye}$ , and  $C_{Ze}$  are defined as

$$C_{Xe} = \frac{F_{Xe}}{\frac{1}{2}\rho A_e U^2} \quad C_{Ye} = \frac{F_{Ye}}{\frac{1}{2}\rho A_e U^2} \quad C_{Ze} = \frac{F_{Ze}}{\frac{1}{2}\rho A_e U^2} \quad (23)$$

The elemental forces  $F_{Xe}$ ,  $F_{Ye}$ , and  $F_{Ze}$  are given by Eqs. (14), (18), and (19). The drag force is the  $Y_A$  component of the total force. Thus, the drag coefficient is expressed as

$$C_D = C_{Fx} \sin \phi \cos \theta + C_{Fy} \cos \phi \cos \theta - C_{Fz} \sin \theta \quad (24)$$

Overall coefficients that define the moments about the body axes are given by

$$C_{Mx} = \sum_{i=1}^I \sum_{j=1}^{J(i)} [C_{ZB} P_{YB} - C_{YB} P_{ZB}]_{ij} (A_{\text{ref}} L_{\text{ref}})^{-1} \quad (25a)$$

$$C_{My} = \sum_{i=1}^I \sum_{j=1}^{J(i)} [C_{XB} P_{ZB} - C_{ZB} P_{XB}]_{ij} (A_{\text{ref}} L_{\text{ref}})^{-1} \quad (25b)$$

$$C_{Mz} = \sum_{i=1}^I \sum_{j=1}^{J(i)} [C_{YB} P_{XB} - C_{XB} P_{YB}]_{ij} (A_{\text{ref}} L_{\text{ref}})^{-1} \quad (25c)$$

where  $P_{XB}$ ,  $P_{YB}$ , and  $P_{ZB}$  define the position of the centroid of a surface element in the body coordinate system [Eq. (4)].

### Skylab Application

A FORTRAN program, based on the methods presented, was developed to promptly obtain the overall aerodynamic coefficients for any spacecraft that can be modeled as a combination of the basic shapes presented in Fig. 2. The program input includes 13 flowfield-computation parameters and, for each basic shape used in the model, 15 position and geometry parameters. Some of the 13 flowfield-computation parameters include the reference area, reference length, average temperature ratio, and molecular speed ratio. The 15 position and geometry parameters include three surface-defining dimensions, a shape identification number, two integers for defining the number of surface divisions, three body components ( $x_0$ ,  $y_0$ , and  $z_0$ ) that define the origin position of a shape's component coordinate system, three angles that locate the  $X_c$  axis of a shape's component system with respect to the  $X_B$ ,  $Y_B$ , and  $Z_B$  axes, and three angles that locate the  $Y_c$  axis in the body system.

A sample application using Skylab is presented to illustrate the program's ability to handle complex configurations. A comparison of the program output with the aerodynamic predictions of a previous Skylab study is presented. Skylab geometry<sup>9</sup> is shown in Fig. 8. The model is composed of 18 shapes including five circular plates, three circular cylinders, three circular cones, six rectangular boxes, and one triangular box. The origin of the body coordinate system is located at the center of gravity as shown in the figure.

The program (given the name FREEMAC)<sup>†</sup> was input along with the Skylab geometry and flowfield data to an IBM 370/3033 computer. For each orientation, approximately 4 s of computer time were required to compute the seven coefficients  $C_D$ ,  $C_{Fx}$ ,  $C_{Fy}$ ,  $C_{Fz}$ ,  $C_{Mx}$ ,  $C_{My}$ , and  $C_{Mz}$ . A total of 2370 surface elements were used in the analysis. Some of the

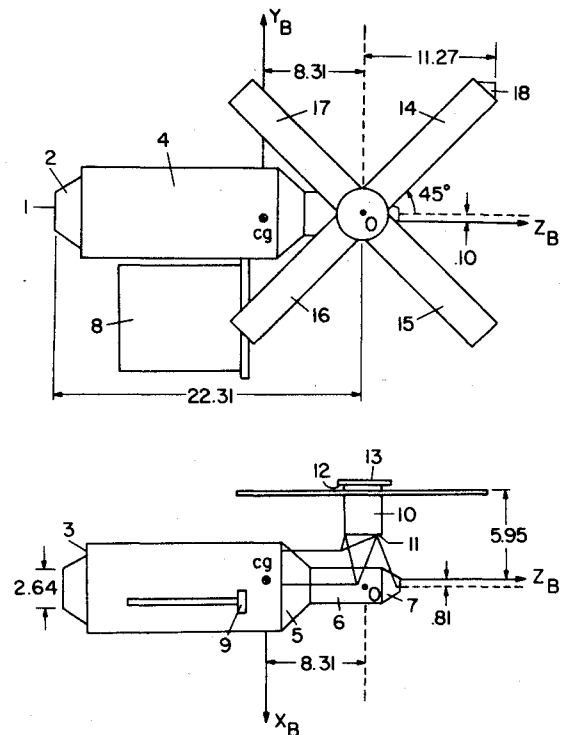


Fig. 8 Model of Skylab geometry.

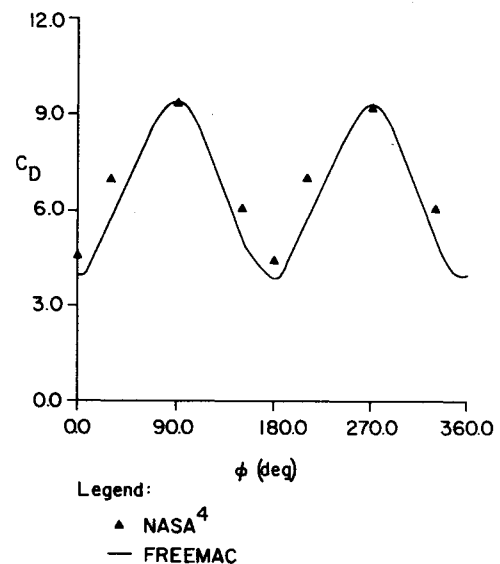


Fig. 9 Skylab drag coefficients for  $\theta = 0$  deg.

results using FREEMAC are compared with previous Skylab results in Figs. 9-13.

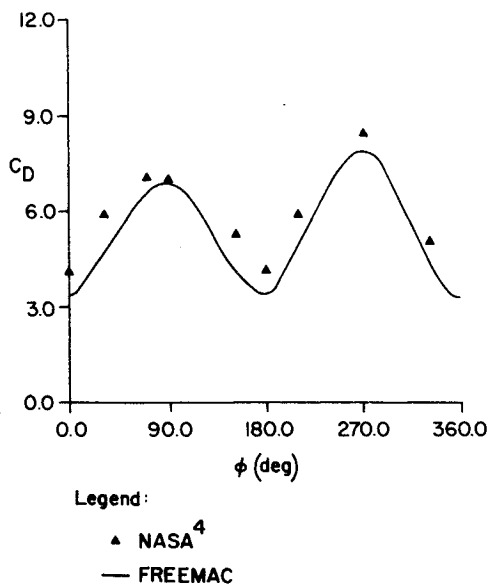
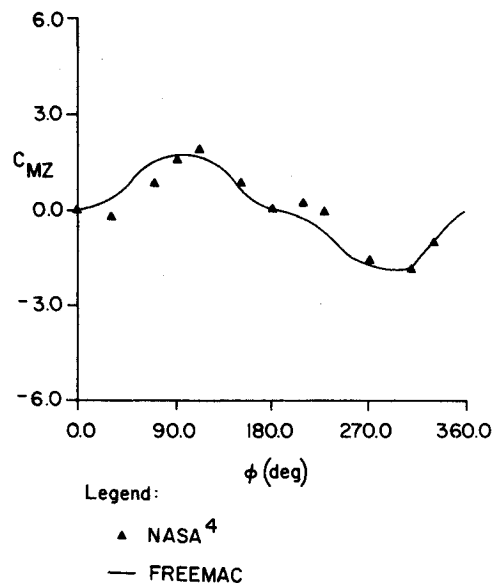
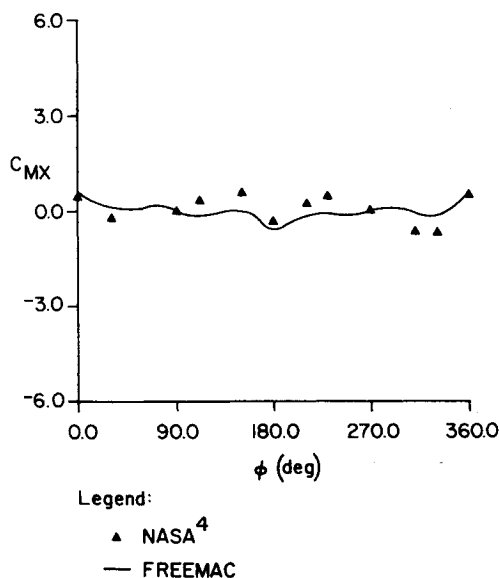
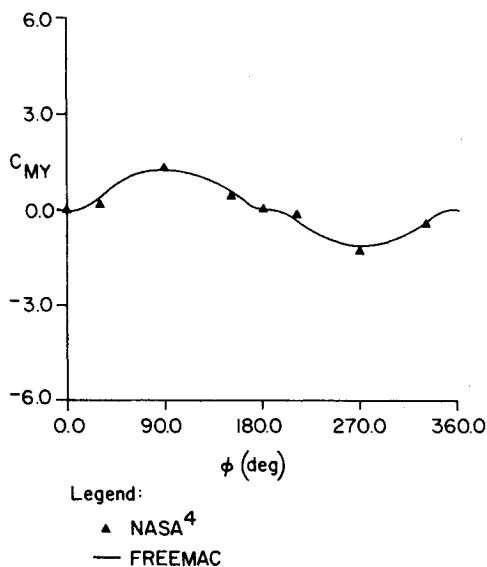
The drag coefficients for  $\theta = 0$  deg and  $0 \text{ deg} \leq \phi \leq 360 \text{ deg}$  are shown in Fig. 9. The difference in the results of FREEMAC and Ref. 4 range from 0% to 10% for the entire set of roll angles. Skylab drag coefficients for  $\theta = 30$  deg and  $0 \text{ deg} \leq \phi \leq 360 \text{ deg}$  are shown in Fig. 10. Again, the FREEMAC results are within 10% of the results of Ref. 4 for most of the roll angles.

Moment coefficients about the  $X_B$ ,  $Y_B$ , and  $Z_B$  axes for  $\theta = 0$  deg and  $0 \text{ deg} \leq \phi \leq 360 \text{ deg}$  are shown in Figs. 11-13. The results of FREEMAC are similar to those of Ref. 4.

### Summary

A numerical procedure to calculate the free-molecular aerodynamic coefficients for complex spacecraft configurations has been presented. The procedure involves the modeling of the spacecraft geometry by numerous basic shapes. The overall aerodynamic coefficients are determined

<sup>†</sup>A listing of FREEMAC is available upon request to the authors.

Fig. 10 Skylab drag coefficients for  $\theta = 30$  deg.Fig. 13 Skylab moment coefficients ( $Z_B$  axis) for  $\theta = 0$  deg.Fig. 11 Skylab moment coefficients ( $X_B$  axis) for  $\theta = 0$  deg.Fig. 12 Skylab moment coefficients ( $Y_B$  axis) for  $\theta = 0$  deg.

by dividing the surfaces of the basic shapes that represent the spacecraft geometry into numerous elemental areas and then summing the force contributions from each exposed element. Surface shielding is accounted for through the use of a shadow-projection technique and simple geometric relationships. Forces on an elemental area are determined by using the gas-surface interaction model of Schaaf and Chambre and the momentum accommodation data of Knechtel and Pitts.

The procedure was formulated as a FORTRAN computer program (FREEMAC) and applied to Skylab. The program was run for the Skylab configuration and output compared with data from a previous study of its aerodynamic behavior. Drag coefficients for both analyses differed by less than 15% for a wide range of orientations. Moment coefficients were also found to be similar. Overall, the Skylab application illustrated the versatility of this procedure in computing coefficients for complex configurations in any orientation.

## References

- <sup>1</sup>Schaaf, S.A. and Chambre, P.L., "Flow of Rarefied Gases," *Fundamentals of Gas Dynamics*, edited by H.W. Emmons, Princeton University Press, Princeton, N.J., 1958, pp. 687-708.
- <sup>2</sup>Meirovitch, L. and Wallace Jr., F.B., "On the Effect of Aerodynamic and Gravitational Torques on the Attitude Stability of Satellites," *AIAA Journal*, Vol. 4, Dec. 1966, pp. 2196-2202.
- <sup>3</sup>Evans, W.J., "Aerodynamic and Radiation Disturbance Torques on Satellites Having Complex Geometry," *Journal of the Astronautical Sciences*, Vol. 9, 1962, pp. 93-99.
- <sup>4</sup>Johnson, J.D., NASA Marshall Space Flight Center, Huntsville, Ala., Internal Memo, Feb. 1979.
- <sup>5</sup>Doughty, R.O. and Schaetzle, W.J., "Experimental Determination of Momentum Accommodation Coefficients at Velocities up to and Exceeding Earth Escape Velocity," *Rarefied Gas Dynamics*, Proceedings of the Sixth International Symposium, edited by L. Trilling and H. Wachman, Academic Press, New York, 1969, pp. 1035-1054.
- <sup>6</sup>Knechtel, E.D. and Pitts, W.C., "Normal and Tangential Momentum Accommodation for Earth Satellite Conditions," *Astronautica Acta*, Vol. 18, No. 3, 1973, pp. 171-184.
- <sup>7</sup>Kaplan, M.H., *Modern Spacecraft Dynamics and Control*, John Wiley and Sons, New York, 1976, Chap. 1.
- <sup>8</sup>Fan, C., "Aerodynamic Forces and Heat Transfer on Shielded Flat Plates in a Free Molecular Flow," *Rarefied Gas Dynamics*, Proceedings of the Sixth International Symposium, edited by L. Trilling and H. Wachman, Academic Press, New York, 1969, pp. 551-560.
- <sup>9</sup>"Skylab Operations Handbook," Amendment 116(07/03/73), NASA MSC-01549, Vol. IV, Rev. A, 1973, pp. 1-8.